EPJ Web of Conferences **21**, 02001 (2012)
DOI: 10.1051/epjconf/20122102001

Asymmetric Fission in the ^{78}Kr+^{40}Ca reactions at 5.5 MeV/nucleon

J.P. Wieleczko[1,a], G. Ademard[1], K. Mazurek[1], C. Schmitt[1], E. Bonnet[1], A. Chbihi[1], J.D. Frankland[1], J. Gomez del Campo[2], M. La Commara[3,4], M. Vigilante[3,4], E. Rosato[3,4], G. Spadaccini[3,4], C. Beck[5], S. Barlini[6], B. Borderie[7], R. Bougault[8] , R. Dayras[9] , G. De Angelis[10], J. De Sanctis[11], V.L. Kravchuk[10], P. Lautesse[12], N. Le Neindre[8] , A. D'Onofrio[14], M. Parlog[8] , D. Pierroutsakou[4], M. Romoli[4], and R. Roy[13]

[1] Grand Accélérateur National d'Ions Lourds (GANIL), CEA/DSM-CNRS/IN2P3, Bvd H. Becquerel, 14076, Caen, France
[2] Physics Division, Oak Ridge National Laboratory, Oak Ridge, TN 37831, USA
[3] Dipartimento di Scienze Fisiche, Università di Napoli "Federico II", I-80126, Napoli, Italy
[4] INFN, Sezione di Napoli, I-80126, Napoli, Italy
[5] IPHC, IN2P3-CNRS and Université Strasbourg, F-67037, Strasbourg Cedex2, France
[6] INFN, Sezione di Firenze, I-50125 Firenze, Italy
[7] IPNO, IN2P3-CNRS and Université Paris-Sud 11, F-91406, Orsay Cedex, France
[8] LPC, IN2P3-CNRS, ENSICAEN and Université, F-14050, Caen Cedex, France
[9] CEA, IRFU, SPhN, CEA/Saclay, F-91191, Gif-sur-Yvette Cedex, France
[10] INFN, LNL, I-35020 Legnaro (Padova) Italy
[11] INFN, Sezione di Bologna, I-40127 Bologna, Italy
[12] IPNL, IN2P3-CNRS et Université, F-69622, Villeurbanne Cedex, France
[13] Laboratoire de Physique Nucléaire, Université de Laval, Québec, Canada
[14] Dipartimento di Scienze Ambientali, Seconda Università di Napoli, I-81100, Caserta, Italy

Abstract. The cross section, kinetic energy distribution and angular distribution of fragments with atomic number $3 \leq Z \leq 28$ emitted in the reaction ^{78}Kr + ^{40}Ca at the bombarding energy of 5.5 MeV/nucleon and coincidence between light charged particles and fragments were measured by means of the 4π-INDRA array to study the decay mechanism of medium mass excited nucleus. Global features indicate a high degree of relaxation and are compatible with a binary fission from compound nucleus. The mean value of the kinetic energy distributions of fragments indicates dominance of Coulomb interaction, while the width of the distribution signals large fluctuations. Inclusive cross-section distributions of fragments with charge $3 \leq Z \leq 28$ are bell-shaped and a strong even-odd-staggering (o-e-s) is observed for $3 \leq Z \leq 12$. Coincidence measurements suggest that the light partners in very asymmetric fission are emitted at excitation energies below the particle emission thresholds. Data were confronted to the predictions of statistical model describing the decay of compound nuclei by emission of light particles and fragments. Calculations assuming spherical fission fragments and finite-range liquid drop fission barriers are not able to explain the experimental features. Attempts have been made to improve the agreement with experimental data. The analysis indicates the strong influence of the shape parameterization of the potential energy surface in describing the fission process of intermediate mass compound nuclei.

[a] e-mail: wieleczko@ganil.fr

1 Introduction

A considerable rearrangement of nuclear matter characterizes a large part of the final states in nuclear collisions. An obvious example of such an evolution is the fusion-fission process. In the fusion phase, after contact the colliding system evolves along the driving potential with large transfer of matter, angular momentum and energy and finally ends up to a mononucleus configuration where most of the degree of freedoms at work have been relaxed. In the fission phase the system evolves in multidimensional space and the motion from saddle do scission configuration depends strongly on the coupling between collectives modes and internal degree of freedoms of the fissioning nucleus. Thus this complex phenomena is one of the wealthy laboratory for exploring systems at extreme deformation associated to dissipative phenomena like diffusion and friction processes.
The region of nucleus with intermediate fissility has very important specificities. The first one is related to the large variety of shapes of the fissioning system along the trajectory from saddle to scission configuration. These shapes vary with the angular momentum or mass (charge)-asymmetry as predicted by various liquid drop models using different shape parameterization and different formulation of the macroscopic part of the binding energy [1–8]. The common results of these approaches is that medium mass compound nuclei have to be strongly deformed to reach scission configuration. The second specificity is the fact that high angular momentum could be transferred into these nuclei without fissioning. For these reasons, the experimental study of the decay modes from medium mass compound nucleus would allows to bring more constraints on the models that aim to describe the fission process.
In a recent work [9] we have reported on the production of fragments in the ^{78}Kr + ^{40}Ca reaction at 5.5 MeV/nucleon. Kinetic energy and angular distributions, cross sections of fragments with atomic number $3 \leq Z \leq 28$ and light-charged particles in coincidence with fragments were measured using the INDRA [10] array. The global features indicate a high degree of relaxation and are compatible with a binary fission from compound nucleus or a long-lived nuclear system. The experimental fragment cross-sections were confronted to various theoretical approaches assuming either the formation of compound nucleus or describing both the collisional stage preceding the compound nucleus formation and the competition with quasifission process. Even thought the better agreement in reproducing the experimental cross-sections is obtained assuming a mixture of fusion-fission and quasifission mechanisms, further study of kinematic observables is needed. Indeed, while charge-(mass) distributions strongly depend on the choice of the potential energy surface [11] near the saddle point configuration, the total kinetic energy releases in the process puts severe constraints on the modeling of both the descent from saddle to scission and to the scission point configuration. In this contribution we will compare both experimental fragment cross-sections and total kinetic energy releases in binary decay to the predictions of the transition-state model [12] assuming the finite-range liquid drop approach extended to the whole charge-(mass) asymmetry degree of freedom [1,2].

2 Experimental details

The experiment was performed at the GANIL facility. Beam of ^{78}Kr projectiles with energy of 5.5 MeV/nucleon impinged on self-supporting ^{40}Ca targets of 1mg/cm^2 in thickness. The targets were prepared from foils of high purity by applying a rolling method. The kinetic energy and atomic number of the ejectiles were measured on an even-by-event basis thanks to the high capabilities of the 4π multidetector INDRA. For the experimental data reported here a large part of the reaction products is emitted from 3° to 45°. In this range, the INDRA array is made of 8 rings comprising detection modules with three layers: a ionization chamber (IC) operated with 50 Torr of C_3F_8 gas; a 300 μm thick silicon detector (Si) and a 14 or 10 cm length CsI(Tl) scintillator. The medium and backward angles from 45° to 176° are covered by 8 rings equipped with IC/CsI(Tl) and IC/Si/Si(Li) modules. The energy calibration of the various layers was obtained by means of alpha particles emitted from a Cf source and from the elastic scattering of projectiles having various *A/q* values (^{75,78,82}Kr^{+12}, ^{75}As^{+12}, ^{50}Cr^{+12}, ^{100}Mo^{+12}) selected with the CIME cyclotron.The kinetic energy of the detected products were deduced from the energy deposited in the IC and Si detectors, corrected for the energy losses in the target as well as in the dead zones of the various detection layers. Energy calibration of the detectors

ensured on accuracy of within 5%.

3 Experimental results

An event-by-event analysis was used to transform the kinetic energy spectra measured in the laboratory into the center-of-mass frame of the reaction. Some examples of experimental kinetic energy distributions in the center-of-mass are reported in Fig. 1 (symbols). The shape of the distributions are very close to a Gaussian with a small asymmetry at low energy for fragments with high Z or a kind of plateau for fragments with low Z. Such distributions are due to various contributions as isotopic distribution, secondary emission from fragments, fluctuations in interaction barriers due to shape fluctuation,etc...These phenomena are difficult to unfold without comparisons with models.
The total kinetic energy (TKE) distribution associated to a fragment with atomic charge Z was deduced from the kinetic energy spectra assuming for sake of simplicity that no particles were emitted before the binary decay and that the measured fragment is the primary one. This slightly differs from the observed correlation between the two biggest fragments Z_1 and Z_2 with $Z_1 \geq Z_2$ contained in an event with an average value $< Z_1 + Z_2 = 54 >$ whatever the fragment Z_1, that corresponds to a value of two charge units below the total available charge (56). Moreover, the study of the coincidence between light charged particles and fragments has shown that no charged particles are emitted from the light partner in case of asymmetric fission, while in symmetric fission both partners are emitters. Thus, by taking into account the emission of particles in the calculation of the TKE would introduce a level of complication, which, regarding the small amount of secondary particles would slightly affect the TKE value. It is worth noticing that the same hypothesis will be assumed for the predicted TKE.

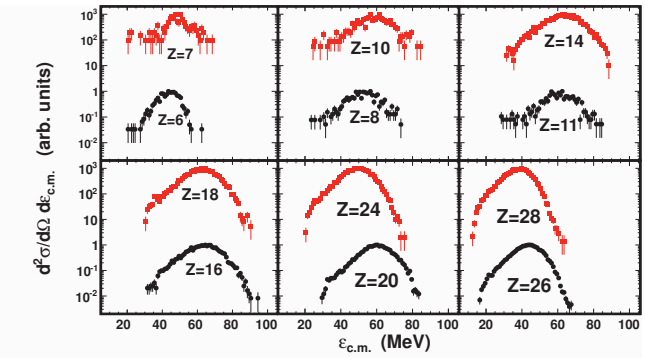

Fig. 1. Center-of-mass kinetic energy distribution of fragments products in the ^{78}Kr + ^{40}Ca reaction at 5.5 MeV/nucleon (red and black symbols).

The experimental mean $< TKE >$ value (circles), the variance $\sigma(TKE)$ (squares) and the ratio $\sigma(TKE)/< TKE >$ (triangles) are reported in Fig. 2 as a function of Z. The mean TKE increases with Z, reaches a maximum at $Z = 20$ and then decreases. This decreasing is at variance with a mechanism dominated by Coulomb interaction in which one would expect an increase of $< TKE >$ up to half of the total available charge, providing that secondary emission from fragments is negligible. The variance $\sigma(TKE)$ of the total kinetic energy distribution is very large and the ratio $\sigma(TKE)/< TKE >$ is roughly constant.
To deepen our characterization of the binary decay, we studied the coincidences between light charged particles (LCPs) and fragments. In a typical event associated to a binary decay, one of the partner is generally detected as well as the LCPs emitted by both partners and possibly by the composite fissioning system. Due to the low excitation energy available in the reaction, the amount of emitted particles is small. Thus, the kick induced by these particles on the residual fragment should be small and it is

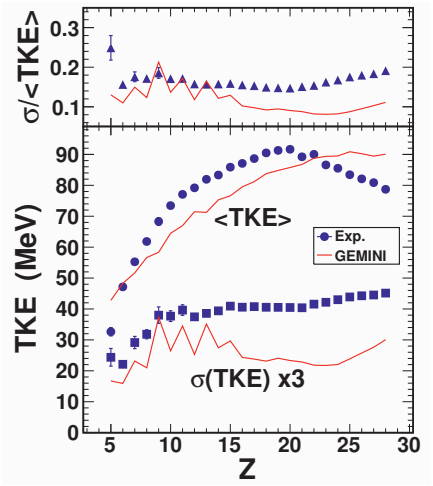

Fig. 2. Experimental mean $< TKE >$ value (circles) , variance $\sigma(TKE)$ (squares) and ratio $\sigma(TKE)/< TKE >$ (triangles) of the total kinetic energy for binary decay measured in ^{78}Kr + ^{40}Ca reaction at 5.5 MeV/nucleon are reported as a function of Z. Note that $\sigma(TKE)$ has been multiply by a factor 3. Comparison with the predictions of GEMINI assuming $< TKE >$ given by equation 2. See text for more details.

reasonable to assume that final fragments left after the secondary emission are flying back-to-back in the center-of-mass. Thus, the emission direction of the light partner defines the recoil direction of its complementary partner. In the present analysis, we calculated for each fragment the relative velocity between that fragment and each detected LCPs in the event. Then we consider a new frame built as follows: one axis is the direction of the fragment velocity in the center-of-mass frame; such a direction together with the beam direction defines a plane ; the direction perpendicular to this plane complete the reference frame. The relative velocities between the fragment and the LCPs are projected onto this new frame. Finally, we obtained the component parallel ($V_{\parallel}$) and perpendicular ($V_{\perp}$) with respect to the direction of the fragment velocity in the c.m. frame. In doing so, for fragments of a given Z emitted at different angles in the c.m., the procedure enables to define a common frame for the LCPs in coincidence with these fragments. With such a procedure applied to an ensemble of reactions, the particles emitted by one fragment of a given Z with a constant velocity value will draw one circle centered at the origin of the reference frame in a $V_{\parallel}$-$V_{\perp}$ diagram.

Fig. 3 presents typical examples of $V_{\parallel} - V_{\perp}$ diagrams for α-Ne (top row, left panel) and α-Fe (top row, right panel) coincidences measured in the ^{78}Kr + ^{40}Ca reaction. The black circles represent the average velocities of emitted α-particles taken from [13]. In case of asymmetric fragmentation, as α-Ne, the relative velocities of the particles fill-in a region akin of a Coulomb ring which is centered at the origin when they are projected into the frame of the complementary partner of the Ne nuclei (top left panel). For almost symmetric fragmentation, as α-Fe, both fragments emit LCPs as illustrated by the two circles centered at both reference frames. A change of behavior is observed in the light-particle emission from asymmetric ($Z = 10$) to almost symmetric ($Z = 26$) fragmentation. The $V_{\parallel} - V_{\perp}$ diagrams for coincidences between α and $Z \leq 10$ show the same feature as the one observed from the α-Ne coincidences. Thus, in ^{78}Kr + ^{40}Ca reactions at 5.5 MeV/nucleon, in the case of symmetric fragmentation both fragments emit LCPs, while for a asymmetric fragmentation, only the heavy fragment emits particles. Obviously, the neutron channel should be considered but it could not be measured by the apparatus used in this experiment. Nevertheless, we have checked that for light fragments the energy thresholds for neutron emission are higher than for LCPs. Consequently, from this analysis, we conclude that the light fragments are produced at excitation energies below the proton or alpha emission thresholds.

As a third piece of information on the binary fragmentation, Fig. 4 presents the cross sections σ_Z for fragments with atomic number 3≤Z≤28 produced in the ^{78}Kr+^{40}Ca reaction at 5.5 MeV/nucleon. The σ_Z distribution exhibits a maximum located at roughly half of the total available charge. σ_Z for frag-

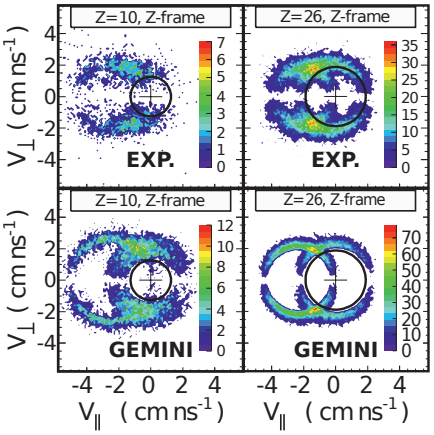

Fig. 3. Experimental $V_{\parallel}$-$V_{\perp}$ diagrams of alpha particles in coincidence with Ne (top row, left panel) and Fe (top row, right panel) fragments measured in the ^{78}Kr + ^{40}Ca reaction at 5.5 MeV/nucleon. Calculated diagrams using the GEMINI code are reported in the bottom row for α-Ne (bottom row, left panel) and α-Fe (bottom row, right panel) coincidences . The black circles represents the average α emission velocity extracted from the Parker's systematics [13].

ments with Z≤10 presents a strong even-odd staggering (e-o-s), and this effect is still seen for higher Z with a smaller amplitude. Staggering of the fragments cross-sections have already been observed in a wide range of energy [14–18] from compound nucleus reactions to spallation and multifragmentation regimes. Moreover, it is worth noting that the *Z*-distribution obtained in the present work is very close to those measured in nuclear systems prepared in roughly the same conditions in terms of excitation energy and angular momentum [19–21] This common features in the yields of the light clusters would indicate that the even-odd staggering observed in the present work is more likely related to the intrinsic properties of light clusters since the heavy complementary partner is different in each system. In our case, emission of fragments with Z≤10 corresponds to asymmetric fission and strong deformation is expected in that phenomenon. Consequently, the observed even-odd-staggering in ^{78}Kr+^{40}Ca reaction would signals the persistence of structure effects in strongly deformed dinuclear system. Due to the low excitation energy deposited in the compound nucleus, three-body final states are unlikely. Thus the measured e-o-s reflects microscopic component on top of macroscopic part of the potential energy surface. Last, it is worth noting that the even-odd-staggering of the cross sections is observed in decay processes involving extreme conditions of temperature [15, 18] and deformation, and thus offers the opportunity to study how the structural properties of nuclei are destroyed or maintained.
In a compound nucleus fission scenario, the three observables quoted above (total kinetic energy, coincidence between LCPs and fragments, fragments cross-sections) provide important information on the whole process, as for example the coupling between collectives and intrinsic degree of freedom, scission configuration, fission barriers, sharing of the excitation energy between partners,etc...We discuss these aspects in the following section by means of a comparison with the predictions of the GEMINI code.

4 Comparison with GEMINI

A global understanding of the many aspects of the compound nuclei decay modes is very challenging and calculations depends on various parameters which could be fixed by confrontation to a variety of experimental observables. The statistical-model code GEMINI describes the light particles and fragment emission by combining the transition-state model extended to the whole charge-(mass) asymmetric degree of freedom [22] and Hauser-Feschbach formalism for particles emission [12]. The barriers for fragment emission (Z ≥ 3) are calculated in the framework of the finite-range liquid-drop model [1]. The level density is calculated within the Fermi gas framework. In the present work the

level-density parameter is taken as $a = A/7MeV^{-1}$. Recent investigation based on extensive analysis of fusion-evaporation data on a wide range of compound nucleus has suggested an energy dependance of the level-density parameter [23]. Using the prescription of that reference would not change drastically our results since the thermal energy is relatively small.

The key input of the model is the distribution of the angular momentum of the compound nucleus. In our experiment we have measured the fusion-evaporation and fusion-fission cross-sections. Assuming a sharp cut-off distribution for the angular momentum, from the total cross-section we deduced $J_{max} = 75$. However, according to the predictions of the finite-range liquid drop model the barriers for symmetric fission of a ^{118}Ba nucleus disappears at $J = 69$. Thus we started the analysis assuming a sharp cut-off distribution with $J_{max} = 69$.

The red histogram in Fig. 4 represents the predictions of GEMINI for the disintegration of ^{118}Ba nucleus. The shape of the Z-distribution for $12 \leq Z \leq 28$ is reasonably reproduced, although σ_Z for $18 \leq Z \leq 26$ are underestimated by roughly 20% which is satisfactory regarding the complexity of the modeling of the fission barriers. More dramatically, the model overestimates by about a factor 10 the integral of the σ_Z cross-sections for $3 \leq Z \leq 11$, the difference coming mainly from the very high Li cross-section, while C and O yields are larger than the experimental ones by about a factor 3. This result does not depend on the sharp cut-off approximation and no major influence is observed by changing the level-density parameter. Finally, the magnitude of the even-odd effect is not at all reproduced for the light fragments. A low barrier for mass-asymmetric fission could explain these features of the Z-distributions for light fragments. For medium-mass nuclei as ^{118}Ba, the total kinetic energy associated to asymmetric fission o is tightly related to the barrier and from the energy balance. Thus, a low potential energy would conversely correspond to high excitation energy in the primary fragments. This could be checked by examining what are the predictions of the model for the coincidence between light particles and fragments.

Calculated $V_{\parallel} - V_{\perp}$ diagrams for α-Ne (bottom row, left panel) and α-Fe (bottom row, right panel) are reported in Fig. 3. In case of asymmetric fission a Coulomb ring is associated to both partners at variance with the experimental data. That means, in the calculations, Ne could be formed from secondary emission of α from fragment with $Z \geq 12$. Thus the excitation energy stored in the light partner in case of asymmetric fission exceeds the particle emission thresholds. For fission close to symmetric fragmentation, the calculated $V_{\parallel} - V_{\perp}$ diagram ressembles to the experimental one, showing two well defined Coulomb rings. However, one observes that the width of the ring is smaller in the calculations which could indicates that the distribution of the relative velocity between LCPs and fragments is broader. Since, in the model, the shape of the partners are assumed to be spherical, the feature of the experimental $V_{\parallel} - V_{\perp}$ diagrams suggests that fragments are deformed.

Last, from Fig. 4 one observes that the calculated cross-sections of light fragments show some staggering. Indeed, we have extracted the primary Z-distribution before secondary decays and we have observed a smooth behavior of the Z-distribution. Thus, the initial shape of the distribution is modified by secondary emission of light-charged particles which induces the fluctuations of the yields. Since, the experimental $V_{\parallel} - V_{\perp}$ diagrams for light fragments do not show such a mechanism of particle emission, one concludes that the experimental e-o-s is not related to secondary emission.

Total kinetic energy distributions of fragments put severe constraint on the scenario under study since they are mainly related to the energy balance at scission configuration. In the model the interaction potential between partner is given by the viola systematics eq. 1

$$E_{viola} = 0.755 \frac{Z_1 Z_2}{(A_1^{1/3} + A_2^{1/3})} + 7.3\ MeV \tag{1}$$

and the total kinetic energy is given as follows :

$$TKE = E_{viola} + E_{rel}(J) \tag{2}$$

In eq. 2, $E_{rel}(J)$ is the energy associated to the relative motion deduced from the rotational saddle configuration

$$E_{rel}(J) = \frac{\mathcal{I}_{rel}}{\mathcal{I}_{sad}} E_{rot,sad}(J) \tag{3}$$

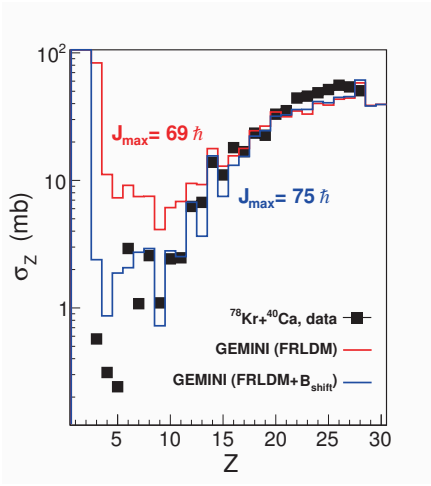

Fig. 4. Experimental cross-sections for fragments (squares) measured in the ^{78}Kr + ^{40}Ca reaction at 5.5 MeV/nucleon. Histograms are the predictions of two calculations performed in the framework of the transition state model [12] assuming the fission barriers given by the FRLDM [1] (red histogram) and by the FRLDM barriers shifted by a constant value $B_{shift} = 7MeV$ (blue histogram). In both cases the level density parameter is taken as $a = A/7MeV^{-1}$. See text for more details.

where $E_{rot,sad}(J)$ is given by

$$E_{rot,sad}(J) = E_{sad}(J) - E_{sad}(0) = \frac{\hbar^2 J(J+1)}{2\mathcal{I}_{sad}} \tag{4}$$

where $E_{sad}(J)$ ($E_{sad}(0)$) is the saddle configuration energy calulated for a given angular momentum J ($J = 0$) respectively which are implemented into the code.
From eq. 4 we deduced I_{sad} and I_{rel} assuming two spheres in contact and the sticking hypothesis for the sharing of the angular momentum.
Red lines in Fig. 2 represent the calculated mean $< TKE >$ value, variance $\sigma(TKE)$ and the ratio $\sigma(TKE)/< TKE >$. The trend of the $< TKE >$ is qualitatively reproduced for $Z \leq 20$ showing that the interaction is dominated by Coulomb interaction. However, the calculated $< TKE >$ underestimates the experimental data by about 10 MeV and does not follow the observed trend above Z=20. A more significant disagreement is observed for the variance which is globally strongly underestimated.
We looked for a possible improvement by introducing a thermal fluctuation deduced from the scission configuration without success. We decided to introduce in the calculation the experimental finding, namely a fluctuation of the TKE such that $\sigma(TKE)/< TKE >$=0.15, an average value close to data. Thus instead of considering a constant value for the TKE we assumed a Gaussian distribution of the TKE centered at $< TKE >$ and with a variance given by $\sigma(TKE)$=0.15$< TKE >$. In doing so, we obviously improved the calculated width but the mean value still disagrees. In the present modeling of the TKE, the only way to increase $< TKE >$ is to increase the contribution from the relative motion, that means increasing the angular momentum.
In a recent investigation on fission process in light and medium mass compound nuclei [24], it has been suggested to introduce a constant shift to the finite-range liquid drop barriers and a value of $B_{shift} = 7MeV$ allows to reproduce the experimental cross-sections of fragments. We introduced the same shift in our calculations. Since the barrier is higher by 7 MeV, the maximum angular momentum that the compound nucleus could sustain increases and indeed, the fission barrier of the ^{118}Ba nucleus disappears at J=75. Thus, the first consequence is a shift of the flux towards higher angular momentum and thus an increasing of the energy associated to the relative motion between partners.
Blue histogram in Fig. 4 represents the new estimation of the fragments cross-sections assuming a shifted profile barriers of 7 MeV with respect to the predictions of the FRLDM. The improvement is spectacular and the shape is globally well reproduced in the whole charge range and more specifically

the cross sections of light fragments are predicted with a right order of magnitude.
A new calculation of the total kinetic energy distribution are presented Fig. 5 and the mean value$< TKE >$, variance $\sigma(TKE)$ and $\sigma(TKE)/< TKE >$ ratio extracted from the kinetic energy distribution are grouped in Fig. 6. The global features are well reproduced, except for $Z \geq 20$. This could be due to deformations of partners which is not included in our simple scenario.

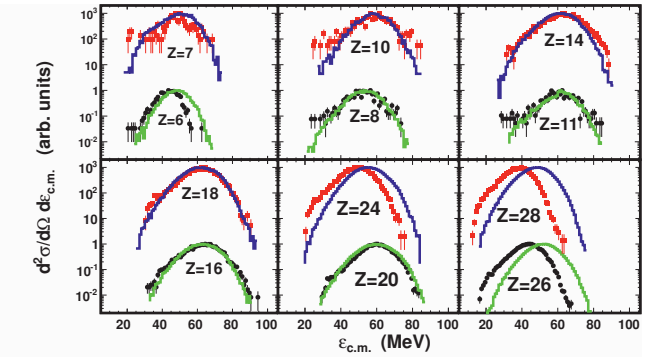

Fig. 5. Experimental kinetic energy distribution in center-of-mass in the ^{78}Kr + ^{40}Ca reaction at 5.5 MeV/nucleon (red and black symbols). Histograms (green and blue) are the predictions of the transition state model, assuming a phenomenological shift B_{shift} of the fission barriers ($B_{shift} = 7MeV$ whatever the charge-(mass) asymmetry) and an empirical fluctuation of the total kinetic energy extracted from data. See text for more details.

5 Summary

Binary decays were investigated in the ^{78}Kr+^{40}Ca reaction at 5.5 MeV/nucleon of bombarding energy. Experimental features of the mechanism at the origin of fragments production are compatible with a disintegration from compound nuclei.
The persistence of structural effects is evidenced from elemental cross-sections. Fragment-particle coincidences show that light fragments are excited below the separation energies of light particles. This finding is also supported by calculations. The first conclusion is that in the the ^{78}Kr+^{40}Ca reaction the even-odd-staggering of the light fragments cross-sections is not predominantly related to the secondary emission of light particles from excited fragments. The second conclusion is that the σ_Z of the light fragments reflects mainly the primary fragmentation and thus they provide important constraints on the energetic balance. The level scheme of the light fragments could also play a role in the final phase space for the decay. Since even-even and odd-odd nuclei have completely different level scheme, one could expect an odd-even-staggering for the yields. Moreover, the collective energy of the configuration governs the phase space which is available for the disintegration, this collective energy should include the properties responsible of the staggering of the yields.
The Z-dependence of the mean total kinetic energy is compatible with a mechanism dominated by the Coulomb interaction between partners. Large fluctuations of the TKE were observed and the ratio $\sigma(TKE)/< TKE >$ is roughly constant. The global features of the kinetic energy distributions are not reproduced assuming a total kinetic energy including both contribution extracted from the Viola systematics and from the relative motion. A fitting procedure assuming a TKE fluctuation given by an average value of the experimental one and a shift of the FRLDM fission barriers by a constant value allows to explain both the Z-distribution over the whole range of charge-asymmetry and the Z-dependence of the $< TKE >$ except for $Z \geq 20$. This feature could be related to deformations of the partners which are observed in the specific pattern of the experimental $V_{\parallel} - V_{\perp}$ diagrams at variance with the calculated one which has been obtained assuming secondary emission from spherical fragments.

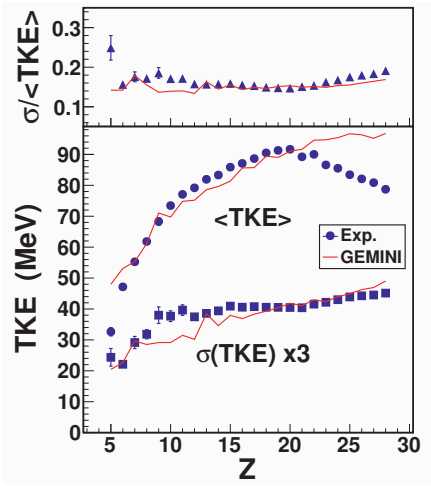

Fig. 6. Experimental mean $< TKE >$ value (circle) , width $\sigma(TKE)$ (square) and ratio $\sigma(TKE)/< TKE >$ (triangle) measured in ^{78}Kr + ^{40}Ca reaction at 5.5 MeV/nucleon are reported as a function of Z. Note that $\sigma(TKE)$ has been multiply by a factor 3. Comparison with the predictions of of the transition state model, assuming a phenomenological shift B_{shift} of the fission barriers ($B_{shift} = 7MeV$ whatever the charge-(mass) asymmetry) and an empirical fluctuation of the total kinetic energy extracted from data. See text for more details.

In the FRLDM approach used for modeling the binary decay in GEMINI, the potential energy surface is calculated assuming three degrees of freedom : elongation, neck and mass-asymmetry. A new version of the FRLDM has been recently proposed in which the deformations of the fragments were included [8,25,26]. Moreover a Wigner term has been included in the calculation of the macroscopic part of the binding energy. This approach seems better suited to explain our data and the shift of the barrier that we have empirically introduced to explain the Z-distribution could be related to the Wigner term. However, our analysis could not be taken as a determination of such a term and comparison with the predictions of the transition state model including this new version of the FRLDM is planned to delineate the relevance of this new parameterization in case of fission of medium mass compound nuclei formed at high angular momentum. This improvement would be of interest also in case of modeling dynamically the descent from saddle to scission by means of Langevin framework. Indeed, various observables relevant to the fission dynamics have been thoroughly studied in the case of binary decay of ^{132}Ce [27], a compound nucleus close to the ^{118}Ba nucleus. While a wide set of observables could be reproduced by the model assuming the time evolution of the system on potential energy surface given by the three dimensions FRLDM, the model fails to explain the TKE distribution with underestimation of the variance by about 40%. It would be interesting to perform such an analysis with the five dimensions FRLDM to verify the availability of the model to explain the large TKE fluctuations or if those fluctuations signal some specific phenomenon related to the rupture of the neck.

References

1. A.J. Sierk, Phys. Rev. Lett. **55**, 582 (1985).
2. A.J. Sierk, Phys. Rev. **C33**, 2039 (1986).
3. M.G. Mustapha,P.A. Baisden, H. Chandra, Phys. Rev. **C25**, 2524 (1982)
4. G. Royer, B. Remaud, Nucl. Phys. **A444**, 472 (1985).
5. S.J.. Sanders, Phys. Rev. **C44**, 2672 (1991)
6. N. Carjan and M. Kaplan, Phys. Rev. **C45**, 2185 (1992) .
7. K. Pomorski and J. Dudek, Phys. Rev. **C67**, 044316 (2003).
8. P. Möller, A.J. Sierk, T. Ichikawa A. Iwamoto, R. Bengtsson, H. Uhrenholt and S. Aberg, Phys. Rev. **C79**, 064304 (2009)

9. G. Ademard *et al.*, Phys. Rev. C**83**, 054619 (2011)
10. J. Pouthas *et al.*, Nucl. Instrum. Methods Phys. Res. **A357**, 418 (1995).
11. K. Mazurek, C. Schmitt, J.P. Wieleczko, P.V. Nadtochy, G. Ademard, Phys. Rev. **C84**, 014611 (2011)
12. R.J. Charity *et al.*, Nucl. Phys. A**476**, 516 (1988).
13. W.E. Parker *et al. Phys. Rev.* **C44**, (1991), 774.
14. S. Steinhaüser *et al.* Nucl. Phys. **A634**, 516 (1998).
15. M.V. Ricciardi, A.V. Ignatyuk, K. Kelic, P. Napolitani, F. Rejmund, K.-H. Schmidt, and O. YordanovNucl. Phys. **A733**, 299 (2004).
16. K.X. Jing, L.G. Moretto, A.C. Veeck, N. Colonna, I. Lhenry, K. Tso, K. Hanold, W. Skulski, Q. Sui, and G.J. Wozniak, Nucl. Phys. **A645**, 203 (1999).
17. T.S. Fan, K.X. Jing, L. Phair, K. Tso, M. McMahan, K. Hanold, G.J. Wozniak, and L.G. Moretto, Nucl. Phys. **A679**, 121 (2000).
18. M.. D'Agostino *et al.* Nucl. Phys. **861**, 47 (2011)
19. L.G. Sobotka *et al.* Phys. Rev. **C36**, 2713 (1987).
20. J. Boger, J.M. Alexander, A. Elmaani, S. Kox, R.A. Lacey, A. Narayanan, D.J. Moses, M.A. McMahan, P.A. DeYoung, and C.J. Gelderloos, Phys. Rev. **C50**, 1006 (1994).
21. E. Vardaci, private communication.
22. L.G. Moretto and G.J. Wozniak, Prog. Part. Nucl. Phys. **21**, 401 (1988).
23. R.J. Charity, Phys. Rev. **C82**, 014610 (2010)
24. D. Mancusi, Proceedings of the International Conference on Fusion, FUSION11, 2-6 May 2011, Saint-Malo.
25. P. Möller, A. Iwamoto, Phys. Rev. **C61**, 047602 (2000)
26. P. Möller, A.J. Sierk and A. Iwamoto, Phys. Rev. Lett. **92**, 072501 (2004)
27. P.N. Nadotchy *et al.*, Proceedings of CNR09, EPJ Web of conferences, **2**, 08003 (2010)